

# A FINITE DIFFERENCE APPROACH TO SOLVING THE TRANSMISSION LINE TELEGRAPH EQUATION

**Christian Y. Cahig \***

Department of Electrical Engineering and Technology  
Mindanao State University - Iligan Institute of Technology  
Iligan City, Philippines  
{christian.cahig}@g.msuiit.edu.ph

## ABSTRACT

Quisque ullamcorper placerat ipsum. Cras nibh. Morbi vel justo vitae lacus tincidunt ultrices. Lorem ipsum dolor sit amet, consectetur adipiscing elit. In hac habitasse platea dictumst. Integer tempus convallis augue. Etiam facilisis. Nunc elementum fermentum wisi. Aenean placerat. Ut imperdiet, enim sed gravida sollicitudin, felis odio placerat quam, ac pulvinar elit purus eget enim. Nunc vitae tortor. Proin tempus nibh sit amet nisl. Vivamus quis tortor vitae risus porta vehicula.

## 1 INTRODUCTION

Consider a transmission line of length  $X$  characterized by per-unit-length series resistance  $R$ , series inductance  $L$ , shunt conductance  $G$ , and shunt capacitance  $C$ . Let  $u(x, t)$  be the instantaneous voltage signal (referred to ground) at point  $x$  along the length of the line at time  $t$ , where  $0 \leq x \leq X$  and  $0 \leq t \leq T$ . We refer to  $x = 0$  as the *sending end* and  $x = X$  as the *receiving end* of the line. From elementary transmission line theory, the propagation of a voltage signal through the line is described by the *telegraph equation*:

$$\frac{1}{LC} \frac{\partial^2 u(x, t)}{\partial x^2} = \frac{\partial^2 u(x, t)}{\partial t^2} + \left( \frac{G}{C} + \frac{R}{L} \right) \frac{\partial u(x, t)}{\partial t} + \left( \frac{RG}{LC} \right) u(x, t) \quad (1)$$

which is a hyperbolic partial differential equation (PDE). Letting

$$c^2 = \frac{1}{LC}, \quad \alpha = \frac{G}{C}, \quad \beta = \frac{R}{L}$$

we can rewrite Equation 1 more succinctly as

$$c^2 \frac{\partial^2 u(x, t)}{\partial x^2} = \frac{\partial^2 u(x, t)}{\partial t^2} + (\alpha + \beta) \frac{\partial u(x, t)}{\partial t} + \alpha \beta u(x, t) \quad (2)$$

The first-order term on the right-hand side of Equation 2 is the *dissipation term*, while the zeroth-order term is the *dispersion term*. In the absence of losses, i.e.,  $R = G = 0$ , the telegraph equation reduces into one describing a wave that propagates at a velocity  $c$  and an angular frequency  $\omega$  given as

$$\omega = \frac{1}{X\sqrt{LC}} \quad (3)$$

Solving the telegraph equation is valuable in the analysis of power system dynamics. However, deriving the expression for the exact analytic solution may not always be tractable nor the most efficient course; in which case numerical approaches that approximate the PDE as a combination of algebraic operations are used. This work presents a basic finite difference method for numerically solving the transmission line telegraph equation.

The remainder of the paper proceeds as follows. Section 2 details how the telegraph equation is approximated as a linear equation via discretization and finite differences. Section 3 presents and discusses results from select worked examples. Section 4 concludes the work.

---

\*Under the supervision of Engr. Michael S. Villame.

## 2 FINITE DIFFERENCE APPROXIMATION

### 2.1 DISCRETIZATION SCHEME

We transform the continuous spatial domain into a set of equally separated discrete points, *i.e.*,

$$0 \leq x \leq X \quad \longrightarrow \quad x_k = k\Delta x, \quad 0 \leq k \leq K \in \mathbb{Z}$$

In other words, we approximate the spatial domain by sampling  $K + 1$  points spaced  $\Delta x$  apart. Note that  $x_0$  corresponds to  $x = 0$  just as  $x_K$  to  $x = X$ . Similarly, for the temporal domain:

$$0 \leq t \leq T \quad \longrightarrow \quad t_n = n\Delta t, \quad 0 \leq n \leq N \in \mathbb{Z}$$

where  $t_0$  corresponds to  $t = 0$  as  $t_N$  to  $t = T$ . The voltage defined on the continuous domain is likewise discretized, and is parametrized by  $k$  and  $n$ :

$$u(x, t) \quad \longrightarrow \quad u(x_k, t_n)$$

For notational convenience,  $u_k^n = u(x_k, t_n)$ .

### 2.2 DIFFERENCE EQUATION

We can approximate the continuous derivatives as central divided differences:

$$\begin{aligned} \frac{\partial u(x, t)}{\partial t} &\longrightarrow \frac{\partial u_k^n}{\partial t} = \frac{u_k^{n+1} - u_k^{n-1}}{2\Delta t} \\ \frac{\partial^2 u(x, t)}{\partial t^2} &\longrightarrow \frac{\partial^2 u_k^n}{\partial t^2} = \frac{u_k^{n+1} - 2u_k^n + u_k^{n-1}}{(\Delta t)^2} \\ \frac{\partial^2 u(x, t)}{\partial x^2} &\longrightarrow \frac{\partial^2 u_k^n}{\partial x^2} = \frac{u_{k+1}^n - 2u_k^n + u_{k-1}^n}{(\Delta x)^2} \end{aligned}$$

Substituting these into their continuous counterparts, we approximate the telegraph as a difference equation:

$$c^2 \frac{u_{k+1}^n - 2u_k^n + u_{k-1}^n}{(\Delta x)^2} = \frac{u_k^{n+1} - 2u_k^n + u_k^{n-1}}{(\Delta t)^2} + (\alpha + \beta) \frac{u_k^{n+1} - u_k^{n-1}}{2\Delta t} + \alpha\beta u_k^n \quad (4)$$

This numerical approximation of Equation 2 suggests that we can estimate the voltage at point  $x_k$  at the next time instant  $t_{n+1}$  given the voltages at  $x_k$  and at the neighbouring points at the current time instant (that is,  $u_k^n$ ,  $u_{k-1}^n$ , and  $u_{k+1}^n$ ) and the voltage at  $x_k$  at the preceding time instant (that is,  $u_k^{n-1}$ ).

### 2.3 UPDATE SCHEME

From Equation 4, we can obtain the “update”  $u_k^{n+1}$  given  $u_k^n$ ,  $u_{k-1}^n$ ,  $u_{k+1}^n$ , and  $u_k^{n-1}$ . To express this more explicitly, we can rewrite Equation 4 as

$$Au_k^{n+1} = Eu_{k-1}^n + Fu_k^n + Eu_{k+1}^n - Bu_k^{n-1} \quad (5)$$

where

$$A = 1 + \frac{\Delta(\alpha + \beta)}{2} \quad (6)$$

$$B = 1 - \frac{\Delta(\alpha + \beta)}{2} \quad (7)$$

$$E = \left(c \frac{\Delta t}{\Delta x}\right)^2 \quad (8)$$

$$F = 2 - 2\left(c \frac{\Delta t}{\Delta x}\right)^2 - \alpha\beta(\Delta t)^2 \quad (9)$$

## 2.4 SOME REMARKS

### 2.4.1 ENCODING INITIAL AND BOUNDARY CONDITIONS

Notice that the difference equation approximation applies for  $k = 1, 2, \dots, K - 1$  and  $n = 1, 2, \dots, N - 1$ . It requires initial (*i.e.*, at  $t_0$ ) and boundary (*i.e.*, at  $x_0$  and  $x_K$ ) values to be specified separately.

In general, initial voltage values are expressed as a function of  $x$ :

$$u(x, 0) = \mu(x) \longrightarrow u_k^0 = \mu(x_k), \forall k.$$

It is also common to have predetermined initial time rate of change of voltage, which can then be approximated by a forward finite divided difference:

$$\frac{\partial u(x, 0)}{\partial t} = \xi^0 \longrightarrow \frac{\partial u_k^0}{\partial t} = \frac{u_k^1 - u_k^0}{\Delta t} = \xi^0 \longrightarrow u_k^1 = u_k^0 + \xi^0 \Delta t, \forall k.$$

The sending- and receiving-end voltages can be expressed as functions of  $t$ :

$$\begin{aligned} u(0, t) &= \nu_0(t) \longrightarrow u_0^n = \nu_0(t_n), \forall n \\ u(X, t) &= \nu_X(t) \longrightarrow u_K^n = \nu_X(t_n), \forall n. \end{aligned}$$

Information at the boundaries may also be expressed in terms of space-derivatives, which can be approximated using forward and backward finite divided differences:

$$\begin{aligned} \frac{\partial u(0, t)}{\partial x} &= \gamma_0 \longrightarrow \frac{\partial u_0^n}{\partial x} = \frac{u_1^n - u_0^n}{\Delta x} = \gamma_0 \longrightarrow u_0^n = u_1^n - \gamma_0 \Delta x, \forall n \\ \frac{\partial u(X, t)}{\partial x} &= \gamma_X \longrightarrow \frac{\partial u_K^n}{\partial x} = \frac{u_K^n - u_{K-1}^n}{\Delta x} = \gamma_X \longrightarrow u_K^n = u_{K-1}^n + \gamma_X \Delta x, \forall n. \end{aligned}$$

### 2.4.2 VECTORIZING THE UPDATE SCHEME

The update scheme Equation 5 is essentially a system of  $K - 1$  linear equations:

$$A \begin{bmatrix} u_1^{n+1} \\ u_2^{n+1} \\ \vdots \\ u_{K-1}^{n+1} \end{bmatrix} = \begin{bmatrix} E & F & E & 0 & \cdots & 0 & 0 & 0 \\ 0 & E & F & E & \cdots & 0 & 0 & 0 \\ \vdots & \vdots & \vdots & \vdots & \ddots & \vdots & \vdots & \vdots \\ 0 & 0 & 0 & 0 & \cdots & E & F & E \end{bmatrix} \begin{bmatrix} u_0^n \\ u_1^n \\ u_2^n \\ \vdots \\ u_{K-1}^n \\ u_K^n \end{bmatrix} - B \begin{bmatrix} 0 & 1 & 0 & \cdots & 0 & 0 \\ 0 & 0 & 1 & \cdots & 0 & 0 \\ \vdots & \vdots & \vdots & \ddots & \vdots & \vdots \\ 0 & 0 & 0 & \cdots & 1 & 0 \end{bmatrix} \begin{bmatrix} u_0^{n-1} \\ u_1^{n-1} \\ u_2^{n-1} \\ \vdots \\ u_{K-1}^{n-1} \\ u_K^{n-1} \end{bmatrix}$$

Letting

$$\begin{aligned} \tilde{\mathbf{u}}^n &= [u_1^n, u_2^n, \dots, u_{K-1}^n]^\top \in \mathbb{R}^{K-1} \\ \mathbf{u}^n &= [u_0^n, u_1^n, \dots, u_{K-1}^n, u_K^n]^\top \in \mathbb{R}^{K+1} \\ \mathbf{E} &= \begin{bmatrix} E & F & E & 0 & \cdots & 0 & 0 & 0 \\ 0 & E & F & E & \cdots & 0 & 0 & 0 \\ \vdots & \vdots & \vdots & \vdots & \ddots & \vdots & \vdots & \vdots \\ 0 & 0 & 0 & 0 & \cdots & E & F & E \end{bmatrix} \in \mathbb{R}^{(K-1) \times (K+1)} \end{aligned} \quad (10)$$

$$\mathbf{B} = B[\mathbf{0} \quad \mathbf{I} \quad \mathbf{0}] \in \mathbb{R}^{(K-1) \times (K+1)} \quad (11)$$

where  $\mathbf{0}$  is an  $(K - 1)$ -vector of zeros and  $\mathbf{I}$  is the identity matrix of size  $(K - 1)$ , the update equations can be expressed compactly as

$$A\tilde{\mathbf{u}}^{n+1} = \mathbf{E}\mathbf{u}^n - \mathbf{B}\mathbf{u}^{n-1} \quad (12)$$

$$\mathbf{u}^{n+1} = \begin{bmatrix} u_0^{n+1} \\ \tilde{\mathbf{u}}^{n+1} \\ u_K^{n+1} \end{bmatrix} \quad (13)$$

where  $u_0^{n+1}$  and  $u_K^{n+1}$  are determined from the boundary conditions.

### 2.4.3 COURANT-FRIEDRICHS-LEVY (CFL) CONDITION

In general, the finer the spatial and temporal domains are discretized, the better  $u_k^n$  approximates  $u(x, t)$ . However, as  $\Delta x$  and  $\Delta t$  get smaller, the number of gridpoints at which  $u(x, t)$  is to be approximated increases, and so does the computational burden. Moreover, a judicious choice of the spatial and temporal steps helps avoid instability (*i.e.*, when the error drastically accumulates). The CFL condition is a commonly used guide for selecting  $\Delta x$  or  $\Delta t$  (given the other):

$$\epsilon = c \frac{\Delta t}{\Delta x} \leq 1 \quad (14)$$

where  $\epsilon$  is called the *CFL number*. In other words, for a particular  $\Delta x$ , the time step should be

$$\Delta t \leq \frac{\Delta x}{c}$$

to avoid an unstable approximation. Intuitively, this upper limit on  $\Delta t$  says that the simulation cannot be incremented any more than the time required for a wave to travel one grid step in space.

## 3 ILLUSTRATIVE EXAMPLES

To supplement the discussion in the preceding sections, we present a few examples that focus on different aspects of the finite difference numerical approximation of the transmission line telegraph equation. We first investigate the benefits of using the vectorized update scheme (Equation 10–13) in Section 3.1. Then, in Sections 3.2 and 3.3, we look into the effects of varying how “fine” the spatial or the temporal domains are discretized. All procedures are accomplished using NumPy (Harris et al., 2020) on an Intel® Core™ i7-10750H with 16GB of RAM. Source codes and related files are available in `illustrative_examples/` within the project repository.

### 3.1 ON VECTORIZATION

Consider the scenario modelled as

$$\frac{\partial^2 u(x, t)}{\partial x^2} = \frac{\partial^2 u(x, t)}{\partial t^2} + 3.00001 \frac{\partial u(x, t)}{\partial t} + 3 \times 10^{-5} u(x, t) \quad (15)$$

where  $0 \leq x \leq 1$ ,  $0 \leq t \leq 1$ , and subject to

$$u(x, 0) = \sin(5\pi x) + 2 \sin(7\pi x), \quad \forall x \quad (16)$$

$$\frac{\partial u(x, 0)}{\partial t} = 0, \quad \forall x \quad (17)$$

$$u(0, t) = 0, \quad \forall t \quad (18)$$

$$u(1, t) = 0, \quad \forall t \quad (19)$$

Ten  $x$ -domain discretizations are examined; we start from  $K + 1 = 100$  grid points and increment by 50. To avoid numerical instability, we use  $\epsilon = 0.10$  to set the corresponding time steps. For each domain discretization, the telegraph equation is solved using both the basic (Equation 5–9) and the vectorized (Equation 10–13) update schemes. Twenty independent runs are performed, where execution times are the metrics of interest. All procedures are documented in `illustrative_examples/on_vectorization/on_vectorization.ipynb`.

Runtimes for the different discretizations and update schemes are summarized in Figure 1. The vectorized update scheme is significantly faster than the naive loop approach, and the speedup gained increases as the domain discretization gets finer. The disparity in the execution times is attributed to NumPy’s support for array-based computing; in fact, one can expect to arrive at similar findings when using other numerical computing tools such as MATLAB® (The MathWorks Inc., 2020). This suggests that, for the same computational resources and time duration, vectorization enables one to iterate and model more scenarios than using the explicit loop-based approach. Henceforth, we will use the vectorized update scheme.

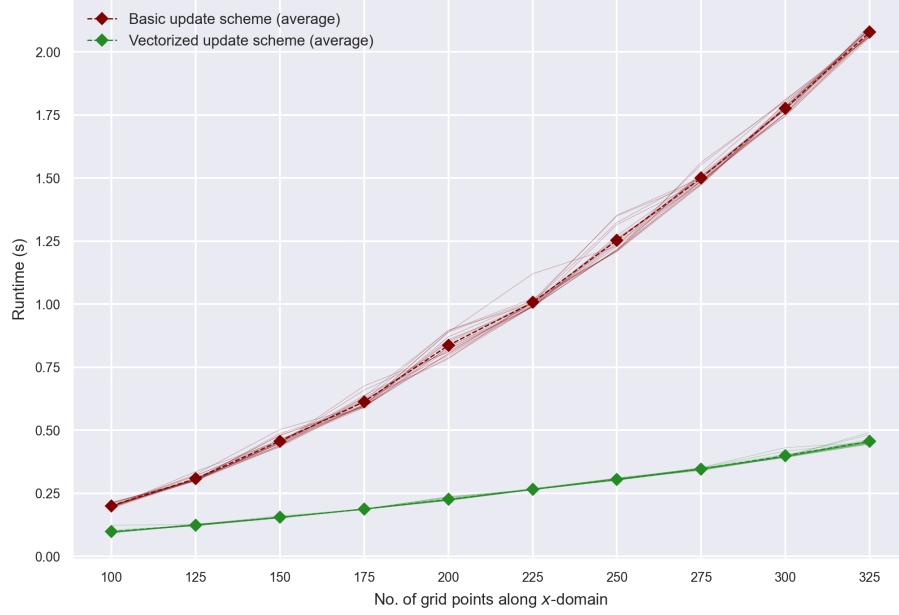


Figure 1: Execution times for basic and vectorized update schemes at different domain discretizations.

### 3.2 ON SPATIAL DOMAIN DISCRETIZATION

Consider the scenario

$$\frac{\partial^2 u(x, t)}{\partial x^2} = \frac{\partial^2 u(x, t)}{\partial t^2} + 3 \frac{\partial u(x, t)}{\partial t} \quad (20)$$

$$u(x, 0) = \sin(5\pi x) + 2 \sin(7\pi x), \quad \forall x \quad (21)$$

$$\frac{\partial u(x, 0)}{\partial t} = 0, \quad \forall x \quad (22)$$

$$u(0, t) = 0, \quad \forall t \quad (23)$$

$$u(1, t) = 0, \quad \forall t \quad (24)$$

where  $0 \leq x \leq 1$  and  $0 \leq t \leq 1$ . From [Zhang et al. \(2019\)](#), the corresponding analytic solution is

$$u(x, t) = e^{-1.5t} \sin(5\pi x) \left[ \cos(\theta(5)t) + \frac{1.5}{\theta(5)} \sin(\theta(5)t) \right] + 2e^{-1.5t} \sin(7\pi x) \left[ \cos(\theta(7)t) + \frac{1.5}{\theta(7)} \sin(\theta(7)t) \right] \quad (25)$$

$$\theta(z) = \sqrt{(z\pi)^2 - 1.5^2} \quad (26)$$

To illustrate how discretization of the spatial domain affects the quality of the numerical approximation, we consider varying  $K$  (and hence, the number of grid points) while fixing  $N = 999$  (that is, 1000 grid points along the temporal domain). We compare the results obtained using the finite difference approximations and those obtained by the analytic solution (Equation 25–26); in particular, we look at the mean squared error (MSE) calculated as

$$\sqrt{\sum_{n=0}^N \sum_{k=0}^K \{u(x_k, t_n) - \hat{u}(x_k, t_n)\}^2}$$

where  $u(x_k, t_n)$  and  $\hat{u}(x_k, t_n)$  are the respective analytic and approximate instantaneous voltages evaluated at the grid points along  $x$ - and  $t$ -domains. All procedures are documented in illustrative examples/on spatial domain discretization/on spatial domain discretization.ipynb.

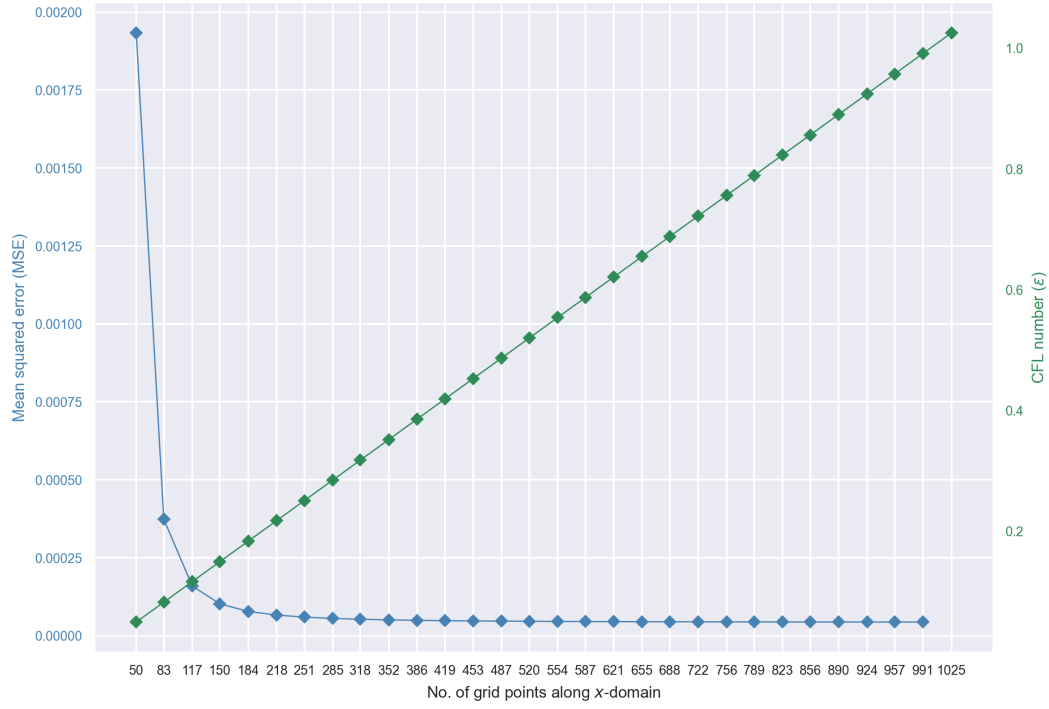


Figure 2: MSE and  $\epsilon$  for various discretization schemes of the  $x$ -domain.

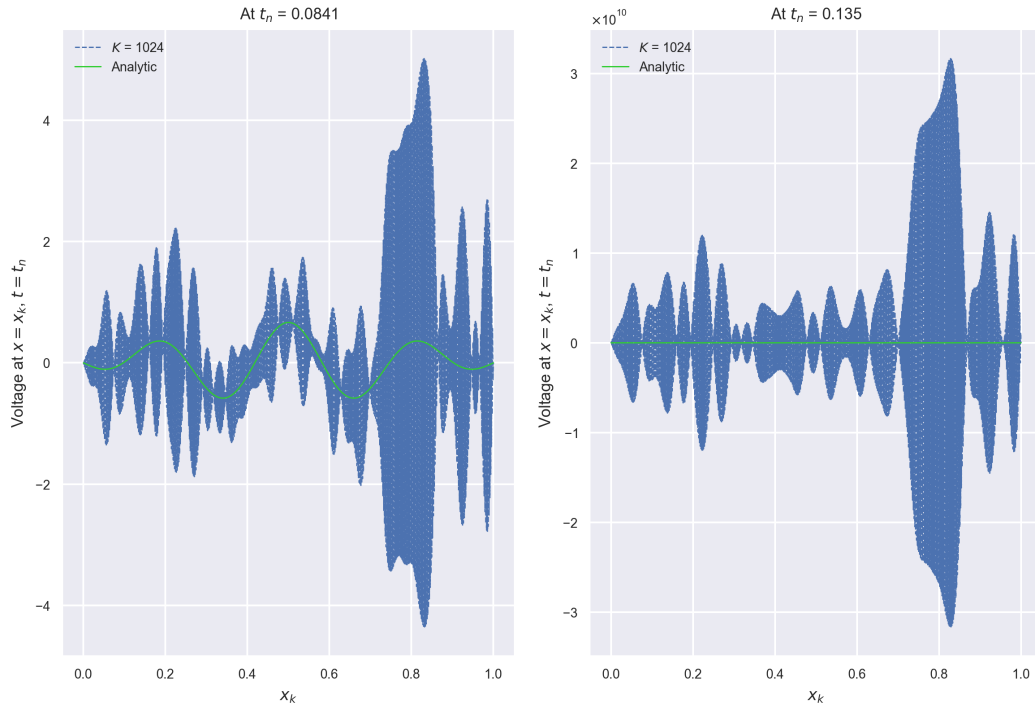


Figure 3: Numerical instability when the  $x$ -domain is approximated by 1025 grid points and the  $t$ -domain by 1000 grid points.

Referring to Figure 2, we find a general trend of the approximation accuracy improving as more grid points are sampled from the spatial domain. One can explain this by considering the limit definition of the partial

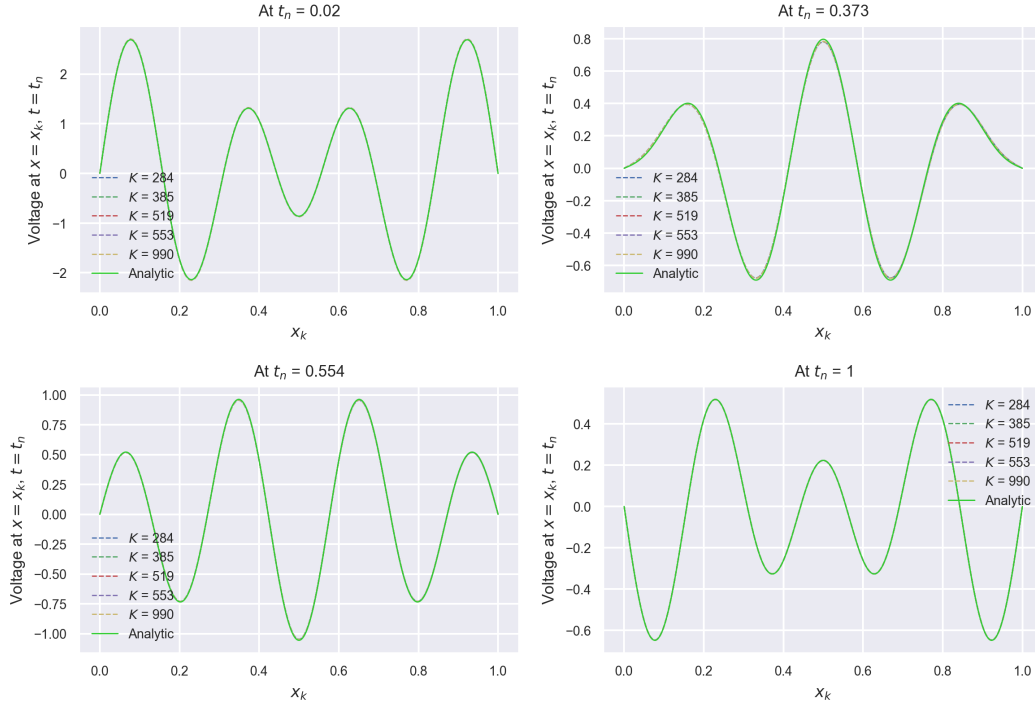


Figure 4: Comparing analytic solution with finite difference approximations at various  $K$ .

derivative with respect to  $x$ :

$$\frac{\partial u(x, t)}{\partial x} = \lim_{\Delta x \rightarrow 0} \frac{u(x + \Delta x, t) - u(x, t)}{\Delta x} \quad (27)$$

Notice also the diminishing returns in accuracy with increasing  $K$ : there is a significant drop in MSE as one increases the number of grid points from 50 to 150, but the improvement tapers off and is insignificant from about 450 to 990 grid points. From a practical viewpoint, one can specify a “good enough” accuracy level so that the number of grid points—and hence, the computational expenses—can be kept to a manageable value. Another salient observation from Figure 2 is that the MSE increases without bounds when 1025 grid points are sampled from the  $x$ -domain. This “finite time blowup” (see Figure 3) is expected to occur since

$$\epsilon = c \frac{\Delta t}{\Delta x} = \frac{1-0}{\frac{1000-1}{1025-1}} = \frac{1024}{999} > 1$$

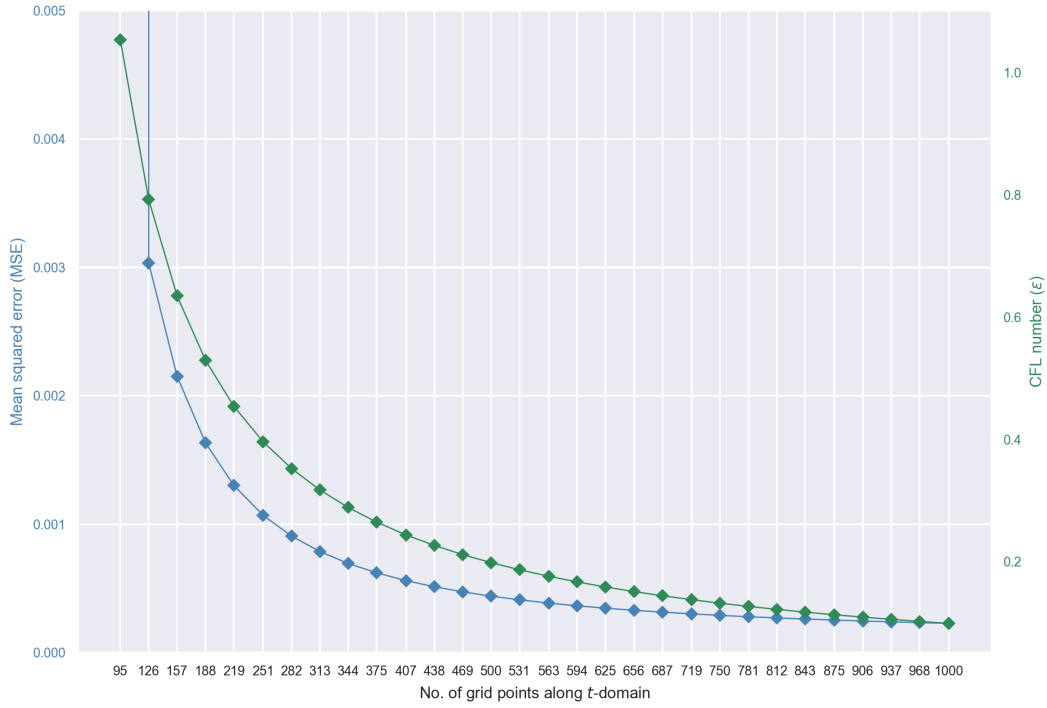
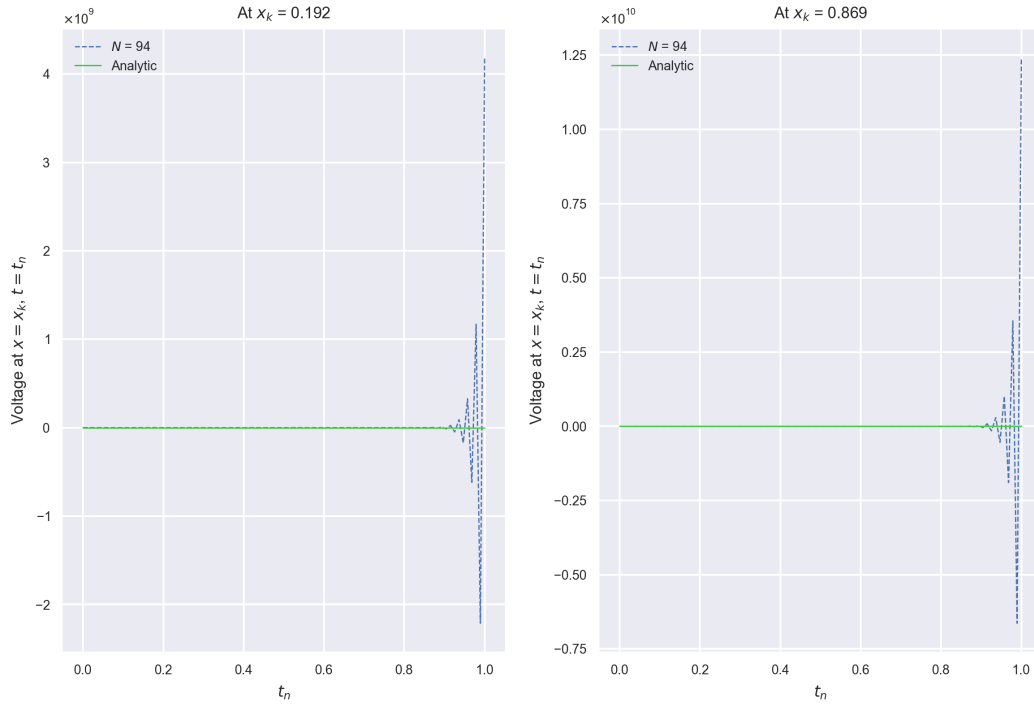
Nevertheless, the finite difference approximation performs well when the number of spatial grid points yields a numerically stable solution (see Figure 4).

### 3.3 ON TEMPORAL DOMAIN DISCRETIZATION

Consider again the scenario in Equation 20–24. This time we illustrate how the discretization of the temporal domain affects the quality of the numerical approximation. Specifically, we vary  $N$  while fixing  $K = 99$  (that is, 100 grid points along the spatial domain). We compare the results obtained using the finite difference approximations and those obtained by the analytic solution (Equation 25–26) in terms of the MSE. All procedures are documented in `illustrative examples/on temporal domain discretization/on temporal domain discretization.ipynb`.

We see in Figure 5 that, for a fixed discretization of the spatial domain, the finite difference approximation generally improves (*i.e.*, the MSE decreases) as more grid points are sampled from the temporal domain. This can be explained by considering the limit definition of the partial time derivative:

$$\frac{\partial u(x, t)}{\partial t} = \lim_{\Delta t \rightarrow 0} \frac{u(x, t + \Delta t) - u(x, t)}{\Delta t} \quad (28)$$

Figure 5: MSE and  $\epsilon$  for various discretization schemes of the  $t$ -domain.Figure 6: Numerical instability when the  $x$ -domain is approximated by 100 grid points and the  $t$ -domain by 95 grid points.

However, we note that even if we decrease  $\Delta t$  to zero (*i.e.*, the continuous limit) the interpolation error is still nonzero; hence, the MSE never quite reaching null. Similar to the case with  $x$ -domain discretization,



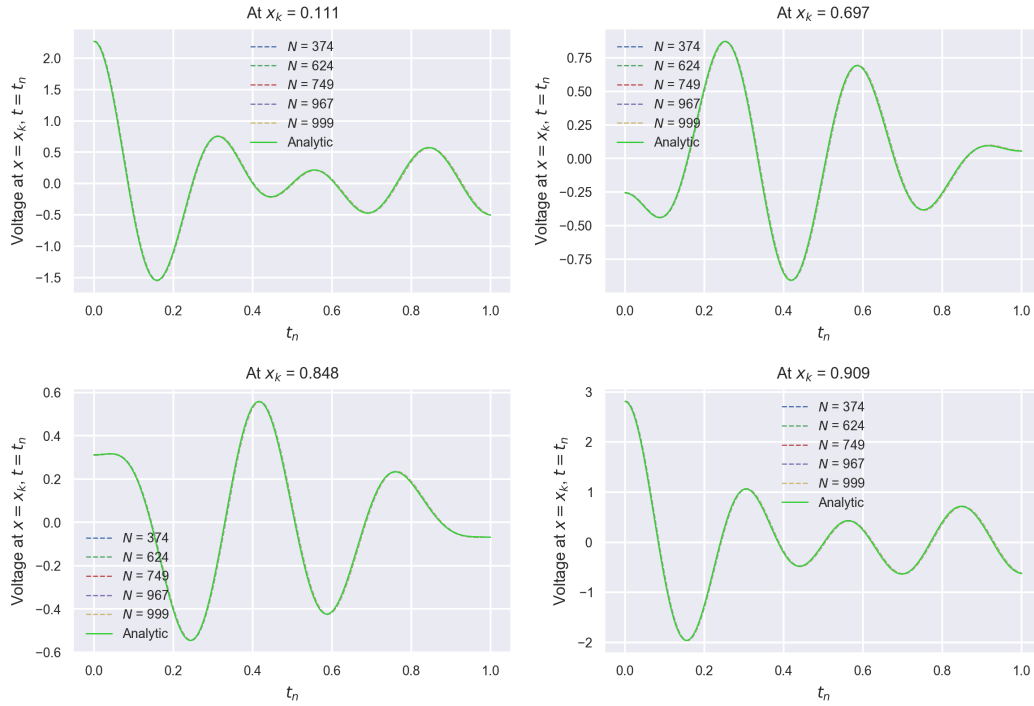


Figure 7: Comparing analytic solution with finite difference approximations at various  $N$ .

the accuracy gain tapers off with increasing  $N$ . From a practical perspective, one can attain approximately the same MSE when using 750 and 1000 grid points, with the former being computationally lighter. We also observe a sudden increase in MSE when 95 grid points are sampled from the  $t$ -domain. This error accumulation, better illustrated in Figure 6, is an expected outcome since

$$\epsilon = c \frac{\Delta t}{\Delta x} = \frac{\frac{1-0}{95-0}}{\frac{1-0}{100-0}} = \frac{100}{95} > 1$$

When the number of temporal grid points yields  $\epsilon \leq 1$ , the finite difference approximation performs well (see Figure 7).

### 3.4 A MULTI-STAGE SCENARIO

Phasellus vestibulum orci vel mauris. Fusce quam leo, adipiscing ac, pulvinar eget, molestie sit amet, erat. Sed diam. Suspendisse eros leo, tempus eget, dapibus sit amet, tempus eu, arcu. Vestibulum wisi metus, dapibus vel, luctus sit amet, condimentum quis, leo. Suspendisse molestie. Duis in ante. Ut sodales sem sit amet mauris. Suspendisse ornare pretium orci. Fusce tristique enim eget mi. Vestibulum eros elit, gravida ac, pharetra sed, lobortis in, massa. Proin at dolor. Duis accumsan accumsan pede. Nullam blandit elit in magna lacinia hendrerit. Ut nonummy luctus eros. Fusce eget tortor.

## 4 CONCLUSION

Nulla ac nisl. Nullam urna nulla, ullamcorper in, interdum sit amet, gravida ut, risus. Aenean ac enim. In luctus. Phasellus eu quam vitae turpis viverra pellentesque. Duis feugiat felis ut enim. Phasellus pharetra, sem id portitor sodales, magna nunc aliquet nibh, nec blandit nisl mauris at pede. Suspendisse risus risus, lobortis eget, semper at, imperdiet sit amet, quam. Quisque scelerisque dapibus nibh. Nam enim. Lorem ipsum dolor sit amet, consectetur adipiscing elit. Nunc ut metus. Ut metus justo, auctor at, ultrices eu, sagittis ut, purus. Aliquam aliquam.

## SUBMISSION OF CONFERENCE PAPERS TO ICLR 2021

ICLR requires electronic submissions, processed by <https://openreview.net/>. See ICLR’s website for more instructions.

If your paper is ultimately accepted, the statement `\iclrfinalcopy` should be inserted to adjust the format to the camera ready requirements.

The format for the submissions is a variant of the NeurIPS format. Please read carefully the instructions below, and follow them faithfully.

### STYLE

Papers to be submitted to ICLR 2021 must be prepared according to the instructions presented here.

Authors are required to use the ICLR  $\text{\LaTeX}$  style files obtainable at the ICLR website. Please make sure you use the current files and not previous versions. Tweaking the style files may be grounds for rejection.

### RETRIEVAL OF STYLE FILES

The style files for ICLR and other conference information are available online at:

<http://www.iclr.cc/>

The file `iclr2021_conference.pdf` contains these instructions and illustrates the various formatting requirements your ICLR paper must satisfy. Submissions must be made using  $\text{\LaTeX}$  and the style files `iclr2021_conference.sty` and `iclr2021_conference.bst` (to be used with  $\text{\LaTeX}2\epsilon$ ). The file `iclr2021_conference.tex` may be used as a “shell” for writing your paper. All you have to do is replace the author, title, abstract, and text of the paper with your own.

The formatting instructions contained in these style files are summarized in sections 4, 4, and 4 below.

### GENERAL FORMATTING INSTRUCTIONS

The text must be confined within a rectangle 5.5 inches (33 picas) wide and 9 inches (54 picas) long. The left margin is 1.5 inch (9 picas). Use 10 point type with a vertical spacing of 11 points. Times New Roman is the preferred typeface throughout. Paragraphs are separated by 1/2 line space, with no indentation.

Paper title is 17 point, in small caps and left-aligned. All pages should start at 1 inch (6 picas) from the top of the page.

Authors’ names are set in boldface, and each name is placed above its corresponding address. The lead author’s name is to be listed first, and the co-authors’ names are set to follow. Authors sharing the same address can be on the same line.

Please pay special attention to the instructions in section 4 regarding figures, tables, acknowledgments, and references.

There will be a strict upper limit of 8 pages for the main text of the initial submission, with unlimited additional pages for citations. Note that the upper page limit differs from last year! Authors may use as many pages of appendices (after the bibliography) as they wish, but reviewers are not required to read these. During the rebuttal phase and for the camera ready version, authors are allowed one additional page for the main text, for a strict upper limit of 9 pages.

### HEADINGS: FIRST LEVEL

First level headings are in small caps, flush left and in point size 12. One line space before the first level heading and 1/2 line space after the first level heading.

#### HEADINGS: SECOND LEVEL

Second level headings are in small caps, flush left and in point size 10. One line space before the second level heading and 1/2 line space after the second level heading.

#### HEADINGS: THIRD LEVEL

Third level headings are in small caps, flush left and in point size 10. One line space before the third level heading and 1/2 line space after the third level heading.

#### CITATIONS, FIGURES, TABLES, REFERENCES

These instructions apply to everyone, regardless of the formatter being used.

#### CITATIONS WITHIN THE TEXT

Citations within the text should be based on the `natbib` package and include the authors' last names and year (with the "et al." construct for more than two authors). When the authors or the publication are included in the sentence, the citation should not be in parenthesis using `\citet{}` (as in "See [Hinton et al. \(2006\)](#) for more information."). Otherwise, the citation should be in parenthesis using `\citep{}` (as in "Deep learning shows promise to make progress towards AI ([Bengio & LeCun, 2007](#)).").

The corresponding references are to be listed in alphabetical order of authors, in the REFERENCES section. As to the format of the references themselves, any style is acceptable as long as it is used consistently.

#### FOOTNOTES

Indicate footnotes with a number<sup>1</sup> in the text. Place the footnotes at the bottom of the page on which they appear. Precede the footnote with a horizontal rule of 2 inches (12 picas).<sup>2</sup>

#### FIGURES

All artwork must be neat, clean, and legible. Lines should be dark enough for purposes of reproduction; art work should not be hand-drawn. The figure number and caption always appear after the figure. Place one line space before the figure caption, and one line space after the figure. The figure caption is lower case (except for first word and proper nouns); figures are numbered consecutively.

Make sure the figure caption does not get separated from the figure. Leave sufficient space to avoid splitting the figure and figure caption.

You may use color figures. However, it is best for the figure captions and the paper body to make sense if the paper is printed either in black/white or in color.

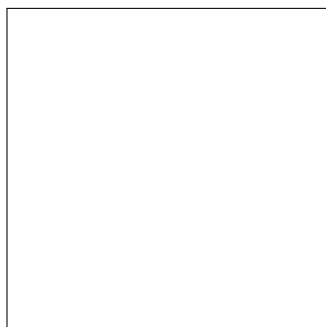


Figure 8: Sample figure caption.

---

<sup>1</sup>Sample of the first footnote

<sup>2</sup>Sample of the second footnote

Table 1: Sample table title

PART	DESCRIPTION
Dendrite	Input terminal
Axon	Output terminal
Soma	Cell body (contains cell nucleus)

## TABLES

All tables must be centered, neat, clean and legible. Do not use hand-drawn tables. The table number and title always appear before the table. See Table 1.

Place one line space before the table title, one line space after the table title, and one line space after the table. The table title must be lower case (except for first word and proper nouns); tables are numbered consecutively.

## DEFAULT NOTATION

In an attempt to encourage standardized notation, we have included the notation file from the textbook, *Deep Learning* Goodfellow et al. (2016) available at [https://github.com/goodfeli/dlbook\\_notation/](https://github.com/goodfeli/dlbook_notation/). Use of this style is not required and can be disabled by commenting out `math_commands.tex`.

### Numbers and Arrays

$a$	A scalar (integer or real)
$\mathbf{a}$	A vector
$\mathbf{A}$	A matrix
$\mathbf{A}$	A tensor
$\mathbf{I}_n$	Identity matrix with $n$ rows and $n$ columns
$\mathbf{I}$	Identity matrix with dimensionality implied by context
$\mathbf{e}^{(i)}$	Standard basis vector $[0, \dots, 0, 1, 0, \dots, 0]$ with a 1 at position $i$
$\text{diag}(\mathbf{a})$	A square, diagonal matrix with diagonal entries given by $\mathbf{a}$
$a$	A scalar random variable
$\mathbf{a}$	A vector-valued random variable
$\mathbf{A}$	A matrix-valued random variable

### Sets and Graphs

$\mathbb{A}$	A set
$\mathbb{R}$	The set of real numbers
$\{0, 1\}$	The set containing 0 and 1
$\{0, 1, \dots, n\}$	The set of all integers between 0 and $n$
$[a, b]$	The real interval including $a$ and $b$
$(a, b]$	The real interval excluding $a$ but including $b$
$\mathbb{A} \setminus \mathbb{B}$	Set subtraction, i.e., the set containing the elements of $\mathbb{A}$ that are not in $\mathbb{B}$
$\mathcal{G}$	A graph
$\text{Pa}_{\mathcal{G}}(\mathbf{x}_i)$	The parents of $\mathbf{x}_i$ in $\mathcal{G}$

### Indexing

$a_i$	Element $i$ of vector $\mathbf{a}$ , with indexing starting at 1
$\mathbf{a}_{-i}$	All elements of vector $\mathbf{a}$ except for element $i$
$A_{i,j}$	Element $i, j$ of matrix $\mathbf{A}$
$\mathbf{A}_{i,:}$	Row $i$ of matrix $\mathbf{A}$
$\mathbf{A}_{:,i}$	Column $i$ of matrix $\mathbf{A}$
$\mathbf{A}_{i,j,k}$	Element $(i, j, k)$ of a 3-D tensor $\mathbf{A}$
$\mathbf{A}_{:,:,i}$	2-D slice of a 3-D tensor
$\mathbf{a}_i$	Element $i$ of the random vector $\mathbf{a}$

### Calculus

$\frac{dy}{dx}$	Derivative of $y$ with respect to $x$
$\frac{\partial y}{\partial x}$	Partial derivative of $y$ with respect to $x$
$\nabla_{\mathbf{x}} y$	Gradient of $y$ with respect to $\mathbf{x}$
$\nabla_{\mathbf{X}} y$	Matrix derivatives of $y$ with respect to $\mathbf{X}$
$\nabla_{\mathbf{x}} y$	Tensor containing derivatives of $y$ with respect to $\mathbf{X}$
$\frac{\partial f}{\partial \mathbf{x}}$	Jacobian matrix $\mathbf{J} \in \mathbb{R}^{m \times n}$ of $f : \mathbb{R}^n \rightarrow \mathbb{R}^m$
$\nabla_{\mathbf{x}}^2 f(\mathbf{x})$ or $\mathbf{H}(f)(\mathbf{x})$	The Hessian matrix of $f$ at input point $\mathbf{x}$
$\int f(\mathbf{x}) d\mathbf{x}$	Definite integral over the entire domain of $\mathbf{x}$
$\int_{\mathbb{S}} f(\mathbf{x}) d\mathbf{x}$	Definite integral with respect to $\mathbf{x}$ over the set $\mathbb{S}$

### Probability and Information Theory

$P(\mathbf{a})$	A probability distribution over a discrete variable
$p(\mathbf{a})$	A probability distribution over a continuous variable, or over a variable whose type has not been specified
$\mathbf{a} \sim P$	Random variable $\mathbf{a}$ has distribution $P$
$\mathbb{E}_{\mathbf{x} \sim P}[f(\mathbf{x})]$ or $\mathbb{E}f(\mathbf{x})$	Expectation of $f(\mathbf{x})$ with respect to $P(\mathbf{x})$
$\text{Var}(f(\mathbf{x}))$	Variance of $f(\mathbf{x})$ under $P(\mathbf{x})$
$\text{Cov}(f(\mathbf{x}), g(\mathbf{x}))$	Covariance of $f(\mathbf{x})$ and $g(\mathbf{x})$ under $P(\mathbf{x})$
$H(\mathbf{x})$	Shannon entropy of the random variable $\mathbf{x}$
$D_{\text{KL}}(P \  Q)$	Kullback-Leibler divergence of $P$ and $Q$
$\mathcal{N}(\mathbf{x}; \boldsymbol{\mu}, \boldsymbol{\Sigma})$	Gaussian distribution over $\mathbf{x}$ with mean $\boldsymbol{\mu}$ and covariance $\boldsymbol{\Sigma}$

### Functions

$f : \mathbb{A} \rightarrow \mathbb{B}$	The function $f$ with domain $\mathbb{A}$ and range $\mathbb{B}$
$f \circ g$	Composition of the functions $f$ and $g$
$f(\boldsymbol{x}; \boldsymbol{\theta})$	A function of $\boldsymbol{x}$ parametrized by $\boldsymbol{\theta}$ . (Sometimes we write $f(\boldsymbol{x})$ and omit the argument $\boldsymbol{\theta}$ to lighten notation)
$\log x$	Natural logarithm of $x$
$\sigma(x)$	Logistic sigmoid, $\frac{1}{1 + \exp(-x)}$
$\zeta(x)$	Softplus, $\log(1 + \exp(x))$
$\ \boldsymbol{x}\ _p$	$L^p$ norm of $\boldsymbol{x}$
$\ \boldsymbol{x}\ $	$L^2$ norm of $\boldsymbol{x}$
$x^+$	Positive part of $x$ , i.e., $\max(0, x)$
$\mathbf{1}_{\text{condition}}$	is 1 if the condition is true, 0 otherwise

## FINAL INSTRUCTIONS

Do not change any aspects of the formatting parameters in the style files. In particular, do not modify the width or length of the rectangle the text should fit into, and do not change font sizes (except perhaps in the REFERENCES section; see below). Please note that pages should be numbered.

## PREPARING POSTSCRIPT OR PDF FILES

Please prepare PostScript or PDF files with paper size “US Letter”, and not, for example, “A4”. The `-t letter` option on `dvips` will produce US Letter files.

Consider directly generating PDF files using `pdflatex` (especially if you are a MiKTeX user). PDF figures must be substituted for EPS figures, however.

Otherwise, please generate your PostScript and PDF files with the following commands:

```
dvips mypaper.dvi -t letter -Ppdf -G0 -o mypaper.ps
ps2pdf mypaper.ps mypaper.pdf
```

## MARGINS IN LATEX

Most of the margin problems come from figures positioned by hand using `\special` or other commands. We suggest using the command `\includegraphics` from the `graphicx` package. Always specify the figure width as a multiple of the line width as in the example below using `.eps` graphics

```
\usepackage[dvips]{graphicx} ...
\includegraphics[width=0.8\linewidth]{myfile.eps}
```

or

```
\usepackage[pdftex]{graphicx} ...
\includegraphics[width=0.8\linewidth]{myfile.pdf}
```

for `.pdf` graphics. See section 4.4 in the graphics bundle documentation (<http://www.ctan.org/tex-archive/macros/latex/required/graphics/grfguide.ps>)

A number of width problems arise when LaTeX cannot properly hyphenate a line. Please give LaTeX hyphenation hints using the `\-` command.

## REFERENCES

- Yoshua Bengio and Yann LeCun. Scaling Learning Algorithms Towards AI. In *Large Scale Kernel Machines*. MIT Press, 2007.
- Ian Goodfellow, Yoshua Bengio, Aaron Courville, and Yoshua Bengio. *Deep Learning*, volume 1. MIT Press, 2016.
- Charles R. Harris, K. Jarrod Millman, Stéfan J. van der Walt, Ralf Gommers, Pauli Virtanen, David Cournapeau, Eric Wieser, Julian Taylor, Sebastian Berg, Nathaniel J. Smith, Robert Kern, Matti Picus, Stephan Hoyer, Marten H. van Kerkwijk, Matthew Brett, Allan Haldane, Jaime Fernández del Río, Mark Wiebe, Pearu Peterson, Pierre Gérard-Marchant, Kevin Sheppard, Tyler Reddy, Warren Weckesser, Hameer Abbasi, Christoph Gohlke, and Travis E. Oliphant. Array programming with NumPy. *Nature*, 585(7825): 357–362, September 2020. doi: 10.1038/s41586-020-2649-2.
- Geoffrey E. Hinton, Simon Osindero, and Yee Whye Teh. A Fast Learning Algorithm for Deep Belief Nets. *Neural Computation*, 18:1527–1554, 2006.
- The MathWorks Inc. *MATLAB R2020b (version 9.9)*. Natick, Massachusetts, 2020.
- Bolong Zhang, Wenjian Yu, and Michael Mascagni. Revisiting Kac’s Method: A Monte Carlo Algorithm for Solving the Telegrapher’s Equations. *Mathematics and Computers in Simulation*, 156:178–193, February 2019. doi: 10.1016/j.matcom.2018.08.007.